

Standard versus generalized chiral perturbation theory: The Chell-Olsson test

M. R. Pennington

Centre for Particle Theory, University of Durham, Durham DH1 3LE, United Kingdom

J. Portolés

INFN, Sezione di Napoli, Dipartimento di Scienze Fisiche, Università di Napoli, I-80125 Napoli, Italy

(Received 10 October 1995; revised manuscript received 4 October 1996)

A way of testing the $\pi\pi$ predictions of chiral perturbation theory against experimental data is to use dispersion relations to continue experimental information into the subthreshold region where the theory should unambiguously apply. Chell and Olsson have proposed a test of the subthreshold behavior of chiral expansions which highlights potential differences between the standard and the generalized forms of the theory. We illustrate how, with current experimental uncertainties, data cannot distinguish between these particular *discriminatory* coefficients despite their sensitivity. Nevertheless, the Chell-Olsson test does provide a consistency check of the chiral expansion, requiring that the $O(p^6)$ corrections to the *discriminatory* coefficients in the standard theory must be $\sim 100\%$. Indeed, some of these have been deduced from the new $O(p^6)$ computations and found to give such large corrections. One can then check that the $O(p^8)$ corrections must be much smaller. We conclude that this test, like others, cannot distinguish between the different forms of chiral symmetry breaking embodied in the alternative versions of chiral perturbation theory without much more precise experimental information near threshold. [S0556-2821(97)01005-9]

PACS number(s): 12.39.Fe

I. INTRODUCTION

The fact that scattering amplitudes are analytic functions means that their behavior at different energy scales is related. Chiral dynamics controls low energy pion reactions and, for instance, requires that the amplitude for $\pi^+\pi^-\rightarrow\pi^0\pi^0$ has a line of real zeros below threshold. This on-shell manifestation of the Adler zero within the Mandelstam triangle, in turn, demands that the $\pi^+\pi^0\rightarrow\pi^+\pi^0$ amplitude must grow asymptotically. Such relationships between the behavior of scattering amplitudes at different energies are naturally embodied in dispersion relations. These can be used as a way of expressing subthreshold amplitudes as integrals over physical region absorptive parts, to be determined either experimentally or theoretically [1]. Chiral perturbation theory (χ PT) allows the same subthreshold quantities to be expressed directly in terms of the parameters of the chiral Lagrangian. There are two realizations of χ PT: Standard ($S\chi$ PT) [2] and generalized ($G\chi$ PT) [3]. In $S\chi$ PT there are two expansion parameters: the momentum squared of an emitted pion and the pion mass characterizing the explicit breaking of chiral symmetry. In $G\chi$ PT the quark condensate matrix element is regarded as an additional dimensionful parameter, in terms of which the standard chiral expansion is reordered. At any finite order either of $S\chi$ PT and $G\chi$ PT may have an expansion with smaller higher order corrections.

The predictions of χ PT can be compared with the evaluation of dispersion relations in two different ways, which depend on the inputs to the dispersive integrals. In an idealized test *A*, the absorptive parts are input wholly from experiment, then the comparison of the subthreshold expansion coefficients with the predictions of χ PT tests the efficacy of the chiral expansion to some given order. Alternatively, in test *B* the absorptive parts are input from χ PT (at least at low energies). Then the comparison tests that the amplitudes of

χ PT satisfy the appropriate analyticity and crossing properties, satisfy unitarity at least perturbatively, and are consistent with experiment for energies beyond where χ PT applies. We will consider these two inequivalent tests in turn.

In 1994, Olsson [4] presented the first of these as a ‘‘stringent test’’ of the chiral expansion schemes, initially reported in the thesis of Chell. Guided by experimental data, Chell and Olsson evaluated the subthreshold expansion coefficients (to be formally defined in Sec. II) using dispersion relations and compared these with the predictions of χ PT in both its standard and generalized forms. While many coefficients evaluated from experiment agreed with both versions of χ PT, several evaluated from experiment were found to be in far better agreement with $G\chi$ PT (with smaller quark condensate) typically by a factor of 2. The results of this test are so intriguing that this issue is worth investigating further.

A number of questions immediately come to mind: (i) does the better agreement with $G\chi$ PT depend on the choice of experimental input? (ii) what is particular about the coefficients that are the basis of this discriminatory test? These questions, among others, are what we answer in this paper. In Sec. II, we define the subthreshold expansion and the dispersive representation of the corresponding coefficients. In Sec. III we give the explicit evaluation of these coefficients at $O(p^4)$ χ PT in its two forms. In Sec. IV we compute dispersively these same coefficients using a flexible parametrization of low energy $\pi\pi$ scattering. We then compare the dispersive and explicit evaluations of the subthreshold coefficients, which allows us to discuss the accuracy of the $O(p^4)$ chiral expansions. We shall see, however, that test *A* is inconclusive because of the sizable experimental uncertainties in the near threshold amplitudes. In Sec. V we turn to test *B*, which checks the consistency of the chiral expansions at any given order. In Sec. VI we present our conclusions.

II. DEFINING THE TESTS

The predictions of χ PT can be verified in two ways. Either the predictions can be continued into the physical regions, where data exist, but then one is uncertain about what energy regime is really appropriate for a given order in χ PT, or, by using dispersion relations, experimental data can be continued below threshold, where χ PT should unambiguously apply. The latter is what we do here by considering the $\pi\pi$ amplitude in the Mandelstam triangle.

To this end, we consider the amplitudes with definite isospin in the t channel: $A^{I_t}(s, t, u)$. From these we construct the functions $\widetilde{F}^{I_t}(\nu, t)$, where

$$\widetilde{F}^{I_t}(\nu, t) = A^{I_t}(s, t, u) \quad \text{for } I_t = 0, 2 \quad (1)$$

and

$$\widetilde{F}^{I_t}(\nu, t) = A^{I_t}(s, t, u)/\nu \quad \text{for } I_t = 1 \quad (2)$$

with

$$\nu = \frac{s-u}{4\mu^2} \quad \text{and} \quad s+t+u=4\mu^2 \quad (3)$$

and $\mu = m_\pi$, the pion mass.¹ The three amplitudes \widetilde{F}^{I_t} are symmetric under $\nu \rightarrow -\nu$.

Now, rather than work with these amplitudes throughout the Mandelstam triangle, it is more convenient to study their Taylor series expansion about the subthreshold point $t=0$, $\nu=0$ (i.e., $s=u=2\mu^2$):

$$\widetilde{F}^{I_t}(\nu, t) = \sum_{k,m} F_{k,m}^{(I_t)} \nu^{2k} t^m, \quad (4)$$

and to study the coefficients $F_{k,m}^{(I_t)}$.

Regge theory leads us to expect that for $|\nu| \rightarrow \infty$ at fixed t ,

$$\widetilde{F}^{I_t=0}(\nu, t) \sim \nu^{\alpha_p(t)}, \quad \text{where } \alpha_p(0) \simeq 1.08,$$

$$\widetilde{F}^{I_t=1}(\nu, t) \sim \nu^{\alpha_\rho(t)-1}, \quad \text{where } \alpha_\rho(0) \simeq 0.5, \quad (5)$$

$$\widetilde{F}^{I_t=2}(\nu, t) \sim \nu^{\alpha_E(t)}, \quad \text{where } \alpha_E(0) < 0.$$

Consequently, $\widetilde{F}^{I_t=1,2}$ satisfy unsubtracted dispersion relations, while that for $\widetilde{F}^{I_t=0}$ requires one subtraction for $t \leq 4\mu^2$. Writing $F^{I_t}(s, t) \equiv \widetilde{F}^{I_t}(\nu, t)$ we have

$$F^{I_t}(s, t) = \frac{1}{\pi} \int_{4\mu^2}^{\infty} ds' \left(\frac{1}{s'-s} + \frac{1}{s'-u} \right) \text{Im} F^{I_t}(s', t), \quad (6)$$

for $I_t = 1, 2$, while

$$\begin{aligned} F^{I_t=0}(s, t) &= F^{I_t=0}(2\mu^2 - t/2, t) \\ &+ \frac{1}{\pi} \int_{4\mu^2}^{\infty} ds' \left(\frac{1}{s'-s} + \frac{1}{s'-u} - \frac{2}{s'-2\mu^2+t/2} \right) \\ &\times \text{Im} F^{I_t=0}(s', t). \end{aligned} \quad (7)$$

We are primarily interested in the subthreshold coefficients, $F_{k,m}^{(I_t)}$, for which the dispersive integral is dominated by the low energy absorptive parts. For $I_t=1, 2$, this means $k+m \geq 1$, while for $I_t=0$ to avoid the dependence on the subtraction term in Eq. (7) also requires at least one derivative with respect to ν^2 , i.e., $k \geq 1$. We, therefore, consider

$$F_{1,0}^{(I_t)} = \frac{8\mu^4}{\pi} \int_{4\mu^2}^{\infty} \frac{ds'}{(s'-2\mu^2)^3} \text{Im} F^{I_t}(s', 0), \quad (8)$$

$$\begin{aligned} \mu^2 F_{1,1}^{(I_t)} &= \frac{4\mu^6}{\pi} \int_{4\mu^2}^{\infty} \frac{ds'}{(s'-2\mu^2)^3} \left(2 \frac{\partial}{\partial t} \text{Im} F^{I_t}(s', t) \Big|_{t=0} \right. \\ &\left. - \frac{3}{s'-2\mu^2} \text{Im} F^{I_t}(s', 0) \right), \end{aligned} \quad (9)$$

$$F_{2,0}^{(I_t)} = \frac{32\mu^8}{\pi} \int_{4\mu^2}^{\infty} \frac{ds'}{(s'-2\mu^2)^5} \text{Im} F^{I_t}(s', 0) \quad (10)$$

for $I_t=0, 1, 2$, and

$$\begin{aligned} \mu^2 F_{0,1}^{(I_t)} &= \frac{\mu^2}{\pi} \int_{4\mu^2}^{\infty} \frac{ds'}{s'-2\mu^2} \left(2 \frac{\partial}{\partial t} \text{Im} F^{I_t}(s', t) \Big|_{t=0} \right. \\ &\left. - \frac{1}{s'-2\mu^2} \text{Im} F^{I_t}(s', 0) \right), \end{aligned} \quad (11)$$

$$\begin{aligned} \mu^4 F_{0,2}^{(I_t)} &= \frac{\mu^4}{\pi} \int_{4\mu^2}^{\infty} \frac{ds'}{4\mu^2 s' - 2\mu^2} \left(\frac{\partial^2}{\partial t^2} \text{Im} F^{I_t}(s', t) \Big|_{t=0} \right. \\ &\left. - \frac{1}{s'-2\mu^2} \frac{\partial}{\partial t} \text{Im} F^{I_t}(s', t) \Big|_{t=0} \right. \\ &\left. + \frac{1}{2(s'-2\mu^2)^2} \text{Im} F^{I_t}(s', 0) \right) \end{aligned} \quad (12)$$

for $I_t=1, 2$.

These form the basis of the Chell-Olsson tests in the forms previously mentioned. Either we input the experimental data for the $\pi\pi$ amplitudes in the dispersive integrals to determine the subthreshold coefficients (test A), or we input the χ PT amplitudes to do so (test B).²

III. EXPLICIT EVALUATION OF SUBTHRESHOLD COEFFICIENTS

We next compute the subthreshold coefficients, defined by Eq. (4), in standard and generalized χ PT based on the

¹Note that this definition of ν differs from that of Chell and Olsson, who use $\nu = (s-u)/4\mu$.

²Of course, test B can only be carried out if the bulk of the contribution to the dispersive integrals comes from the very low energy region where χ PT safely applies. As we will see, this is the case for the so called *discriminatory* coefficients.

formulas of Refs. [2,3] for the $O(p^4)$ $\pi\pi$ amplitudes. We obtain the following.

$S\chi\text{PT}$

$I_t=0$:

$$F_{1,0}^{(0)} = \frac{1}{18\,432\pi^3} \left(\frac{\mu}{F_\pi}\right)^4 [476 - 183\pi + 96(\bar{\mathcal{L}}_1 + 4\bar{\mathcal{L}}_2)], \quad (13)$$

$$\mu^2 F_{1,1}^{(0)} = \frac{1}{8192\pi^3} \left(\frac{\mu}{F_\pi}\right)^4 [88 - 61\pi], \quad (14)$$

$$F_{2,0}^{(0)} = \frac{1}{24\,576\pi^3} \left(\frac{\mu}{F_\pi}\right)^4 [608 - 135\pi], \quad (15)$$

$I_t=1$:

$$F_{1,0}^{(1)} = \frac{7}{18\,432\pi^3} \left(\frac{\mu}{F_\pi}\right)^4 [8 + 3\pi], \quad (16)$$

$$\mu^2 F_{0,1}^{(1)} = \frac{1}{36\,864\pi^3} \left(\frac{\mu}{F_\pi}\right)^4 [76 - 87\pi + 96(\bar{\mathcal{L}}_2 - \bar{\mathcal{L}}_1)], \quad (17)$$

$$\mu^2 F_{1,1}^{(1)} = \frac{1}{73\,728\pi^3} \left(\frac{\mu}{F_\pi}\right)^4 [64 - 93\pi], \quad (18)$$

$$F_{2,0}^{(1)} = \frac{1}{368\,640\pi^3} \left(\frac{\mu}{F_\pi}\right)^4 [512 + 75\pi], \quad (19)$$

$$\mu^4 F_{0,2}^{(1)} = \frac{1}{163\,840\pi^3} \left(\frac{\mu}{F_\pi}\right)^4 [328 - 45\pi], \quad (20)$$

$I_t=2$:

$$F_{1,0}^{(2)} = \frac{1}{18\,432\pi^3} \left(\frac{\mu}{F_\pi}\right)^4 [51\pi - 76 + 96(\bar{\mathcal{L}}_1 + \bar{\mathcal{L}}_2)], \quad (21)$$

$$\mu^2 F_{0,1}^{(2)} = \frac{1}{32\pi} \left(\frac{\mu}{F_\pi}\right)^2 \left\{ -1 + \frac{1}{1152\pi^2} \left(\frac{\mu}{F_\pi}\right)^2 \right. \\ \left. \times [130 + 39\pi - 192\bar{\mathcal{L}}_2 - 144\bar{\mathcal{L}}_4] \right\}, \quad (22)$$

$$\mu^2 F_{1,1}^{(2)} = \frac{-1}{8192\pi^3} \left(\frac{\mu}{F_\pi}\right)^4 [8 + 19\pi], \quad (23)$$

$$F_{2,0}^{(2)} = \frac{1}{24\,576\pi^3} \left(\frac{\mu}{F_\pi}\right)^4 [32 + 27\pi], \quad (24)$$

$$\mu^4 F_{0,2}^{(2)} = \frac{1}{491\,520\pi^3} \left(\frac{\mu}{F_\pi}\right)^4 [160(\bar{\mathcal{L}}_1 + 5\bar{\mathcal{L}}_2) - 468 - 75\pi]. \quad (25)$$

In Eqs. (13)–(25) $\bar{\mathcal{L}}_1$, $\bar{\mathcal{L}}_2$, and $\bar{\mathcal{L}}_4$ are effective coupling constants that appear in the polynomial part of the $O(p^4)$ chiral Lagrangian in $S\chi\text{PT}$ [2].

$G\chi\text{PT}$

$I_t=0$:

$$F_{1,0}^{(0)} = \frac{\mu^4}{9} (120\alpha_0 + 16\beta_0) + \frac{3\beta^2}{\pi(96\pi F_\pi^2)^2} \\ \times \left\{ (8 - 2\pi)\kappa_0^2 + \left(10 - \frac{5}{2}\pi\right)\kappa_2^2 + 8\pi\mu^2\kappa_0 \right. \\ \left. + 10\pi\mu^2\kappa_2 + (112 + 4\pi)\mu^4 \right\}, \quad (26)$$

$$\mu^2 F_{1,1}^{(0)} = \frac{3}{8\pi} \frac{\beta^2}{(96\pi F_\pi^2)^2} \{ (32 - 12\pi)\kappa_0^2 + (40 - 15\pi)\kappa_2^2 \\ - 64\mu^2\kappa_0 - 80\mu^2\kappa_2 - (120\pi + 96)\mu^4 \}, \quad (27)$$

$$F_{2,0}^{(0)} = \frac{1}{8\pi} \frac{\beta^2}{(96\pi F_\pi^2)^2} \{ (128 - 36\pi)\kappa_0^2 + (160 - 45\pi)\kappa_2^2 \\ + 48\pi\mu^2\kappa_0 + 60\pi\mu^2\kappa_2 + (1152 - 72\pi)\mu^4 \}, \quad (28)$$

$I_t=1$:

$$F_{1,0}^{(1)} = \frac{1}{4\pi} \frac{\beta^2}{(96\pi F_\pi^2)^2} \{ (24\pi - 64)\kappa_0^2 + (40 - 15\pi)\kappa_2^2 \\ + 128\mu^2\kappa_0 - 80\mu^2\kappa_2 + (96\pi - 128)\mu^4 \}, \quad (29)$$

$$\mu^2 F_{0,1}^{(1)} = \frac{4}{3}\mu^4\beta_0 + \frac{\beta^2}{\pi(96\pi F_\pi^2)^2} \\ \times \left\{ (3\pi - 12)\kappa_0^2 + \frac{15}{8}(4 - \pi)\kappa_2^2 - 12\pi\mu^2\kappa_0 \right. \\ \left. + \frac{15}{2}\pi\mu^2\kappa_2 - (20 + 6\pi)\mu^4 \right\}, \quad (30)$$

$$\mu^2 F_{1,1}^{(1)} = \frac{1}{16\pi} \frac{\beta^2}{(96\pi F_\pi^2)^2} \{ (9\pi - 32)(8\kappa_0^2 - 5\kappa_2^2) \\ + 12\pi\mu^2(5\kappa_2 - 8\kappa_0) + 16\mu^4(3\pi - 28) \}, \quad (31)$$

$$F_{2,0}^{(1)} = \frac{1}{80\pi} \frac{\beta^2}{(96\pi F_\pi^2)^2} \{ (45\pi - 128)(8\kappa_0^2 - 5\kappa_2^2) \\ + 128\mu^2(8\kappa_0 - 5\kappa_2) + 64\mu^4(15\pi - 32) \}, \quad (32)$$

$$F_{0,2}^{(1)} = \frac{3}{320\pi} \frac{\beta^2}{(96\pi F_\pi^2)^2} \{ 5(3\pi - 8)(8\kappa_0^2 - 5\kappa_2^2) \\ + 80\mu^2(8\kappa_0 - 5\kappa_2) + 768\mu^4 \}, \quad (33)$$

$I_t=2$:

$$F_{1,0}^{(2)} = \frac{8}{9}\mu^4(6\alpha_0 - \beta_0) + \frac{3\beta^2}{4\pi(96\pi F_\pi^2)^2} \{ (4 - \pi)(8\kappa_0^2 + \kappa_2^2) \\ + 4\pi\mu^2(8\kappa_0 + \kappa_2) + 64(1 + \pi)\mu^4 \}, \quad (34)$$

$$\begin{aligned} \mu^2 F_{0,1}^{(2)} = & -\frac{\mu^2}{3} \beta_2 - \frac{8}{9} \mu^4 (3\alpha_0 + \beta_0) - \frac{\beta \mu^2}{32\pi F_\pi^2} \\ & + \frac{3\beta^2}{\pi(96\pi F_\pi^2)^2} \left\{ (2-\pi)\kappa_0^2 + \frac{1}{8}(6-\pi)\kappa_2^2 \right. \\ & \left. - \mu^2(\kappa_2 + 8\kappa_0) + 4(\pi-6)\mu^4 \right\}, \end{aligned} \quad (35)$$

$$\begin{aligned} \mu^2 F_{1,1}^{(2)} = & \frac{3}{16\pi} \frac{\beta^2}{(96\pi F_\pi^2)^2} \{ (8-3\pi)(8\kappa_0^2 + \kappa_2^2) \\ & - 16\mu^2(8\kappa_0 + \kappa_2) - 96(2+\pi)\mu^4 \}, \end{aligned} \quad (36)$$

$$\begin{aligned} F_{2,0}^{(2)} = & \frac{1}{16\pi} \frac{\beta^2}{(96\pi F_\pi^2)^2} \{ (32-9\pi)(8\kappa_0^2 + \kappa_2^2) \\ & + 12\pi\mu^2(8\kappa_0 + \kappa_2) + 288\pi\mu^4 \}, \end{aligned} \quad (37)$$

$$\begin{aligned} \mu^4 F_{0,2}^{(2)} = & \frac{\mu^4}{6} (6\alpha_0 + \beta_0) + \frac{3}{320\pi} \frac{\beta^2}{(96\pi F_\pi^2)^2} \{ 40(4-\pi)\kappa_0^2 \\ & + (36-5\pi)\kappa_2^2 + 160\pi\mu^2\kappa_0 + 20(16+\pi)\mu^2\kappa_2 \\ & + 1280\mu^4 \}. \end{aligned} \quad (38)$$

In Eqs. (26)–(38) α_0 , β_0 , and β_2 are parameters that depend on α , β , and subtraction constants in the dispersive analysis of Stern *et al.* [3], while

$$\kappa_0 \doteq \left(\frac{5\alpha}{6\beta} - \frac{4}{3} \right) \mu^2, \quad \kappa_2 \doteq - \left(\frac{2\alpha}{3\beta} + \frac{4}{3} \right) \mu^2. \quad (39)$$

As an aside, we note that the subthreshold coefficients, Eq. (4), are not, in fact, independent. While their definition embodies the $s-u$ symmetry of the amplitudes (as in πK or πN scattering), the $\pi\pi$ process actually has three-channel crossing. This means that the three isospin amplitudes can each be written in terms of one function, e.g., the Chew-Mandelstam invariant amplitude $A(s, t, u)$. This imposes conditions among the $F_{k,m}^{(I)}$. For instance,

$$\begin{aligned} F_{0,0}^{(2)} = & \frac{1}{3} (F_{0,0}^{(0)} - F_{0,0}^{(2)}) + \frac{4}{3} (F_{0,1}^{(0)} - F_{0,1}^{(2)}) + \frac{8}{3} (F_{0,2}^{(0)} - F_{0,2}^{(2)}) \\ & + \frac{1}{6} (F_{1,0}^{(0)} - F_{1,0}^{(2)}) + \frac{1}{24} (F_{2,0}^{(0)} - F_{2,0}^{(2)}) \\ & + \sum_{k,m>2} c_{k,m} (F_{k,m}^{(0)} - F_{k,m}^{(2)}), \end{aligned} \quad (40)$$

$$\begin{aligned} F_{0,1}^{(2)} = & -\frac{1}{3} (F_{0,1}^{(0)} - F_{0,1}^{(2)}) - \frac{4}{3} (F_{0,2}^{(0)} - F_{0,2}^{(2)}) - \frac{1}{4} (F_{1,0}^{(0)} - F_{1,0}^{(2)}) \\ & - \frac{1}{8} (F_{2,0}^{(0)} - F_{2,0}^{(2)}) + \sum_{k,m>2} d_{k,m} (F_{k,m}^{(0)} - F_{k,m}^{(2)}). \end{aligned} \quad (41)$$

In S χ PT, $\mu^2 F_{0,1}^{(2)} = -2.6 \times 10^{-2}$, while the $k+m \leq 2$ terms in Eq. (41) give -2.7×10^{-2} . In contrast for $F_{0,0}^{(2)}$ Eq. (40), S χ PT gives 5.0×10^{-2} , whereas the $k+m \leq 2$ terms give 6.6×10^{-2} . So these relationships from three-channel cross-

ing are not, in practice, very useful, since they require connections between a large number of coefficients: relationships that are, of course, automatically satisfied by any crossing symmetric representation, like that of χ PT.

Of the coefficients listed in Eqs. (13)–(25), we see in S χ PT that, apart from $F_{1,0}^{(0,2)}$, $F_{0,1}^{(1)}$, $F_{0,1}^{(2)}$, and $F_{0,2}^{(2)}$, the others do not depend on the $\bar{\mathcal{L}}_i$, which specify the polynomial (resonance generated) $O(p^4)$ corrections to the chiral Lagrangian. Contrastingly [2], the $I=0$ S -wave scattering length

$$\begin{aligned} a_0^0 = & \frac{7\mu^2}{32\pi F_\pi^2} \left\{ 1 + \frac{5}{84\pi^2} \left(\frac{\mu}{F_\pi} \right)^2 \left[\bar{\mathcal{L}}_1 + 2\bar{\mathcal{L}}_2 - \frac{3}{8}\bar{\mathcal{L}}_3 \right. \right. \\ & \left. \left. + \frac{21}{10}\bar{\mathcal{L}}_4 + \frac{21}{8} \right] \right\} \end{aligned} \quad (42)$$

on which, as we shall see, the dispersive integrals crucially depend, does involve the $\bar{\mathcal{L}}_i$. In G χ PT at $O(p^4)$, the coefficients all depend on α, β , as does a_0^0 , Eqs. (26)–(39) [5], in the following way:

$$\begin{aligned} a_0^0 = & \frac{\mu^2}{96\pi F_\pi^2} \left\{ (5\alpha + 16\beta) \left(1 + \frac{\mu^2}{48\pi^2 F_\pi^2} (5\alpha + 16\beta) \right) \right. \\ & \left. + 60 \left(\frac{\mu}{F_\pi} \right)^2 (\lambda_1 + 2\lambda_2) \right\}, \end{aligned} \quad (43)$$

where λ_1 and λ_2 can be written in terms of the $\bar{\mathcal{L}}_i$'s of S χ PT as

$$\lambda_1 = \frac{1}{48\pi^2} \left(\bar{\mathcal{L}}_1 - \frac{4}{3} \right), \quad \lambda_2 = \frac{1}{48\pi^2} \left(\bar{\mathcal{L}}_2 - \frac{5}{6} \right). \quad (44)$$

We now evaluate the subthreshold coefficients $F_{k,m}^{(I)}$ using the following set of parameters:³

$$\bar{\mathcal{L}}_1 = -1.1, \quad \bar{\mathcal{L}}_2 = 5.7, \quad (45)$$

$$\bar{\mathcal{L}}_3 = 2.9, \quad \bar{\mathcal{L}}_4 = 1.6,$$

for S χ PT. As is well known, if $\alpha = \beta = 1$ the $O(p^2)$ G χ PT is identical to its standard form. This remains approximately true at higher orders if $\alpha \approx 1$, $\beta \approx 1$. In G χ PT, while β is always close to 1, α is roughly between 1 and 4 depending on the magnitude of the quark condensate. Since we want to compare and, in particular, contrast the two versions of χ PT, we here take G χ PT to have (see footnote 3)

$$\begin{aligned} \alpha = & 3.1, \quad \beta = 0.93, \\ \alpha_0 \mu^4 = & 5.5 \times 10^{-4}, \quad \beta_0 \mu^4 = 3.5 \times 10^{-3}, \\ \beta_2 \mu^2 = & 1.6 \times 10^{-3}. \end{aligned} \quad (46)$$

In columns 2 and 3 of Table I, we list the values of the subthreshold coefficients determined by S χ PT and G χ PT as

³These are the values of the parameters for S χ PT and G χ PT quoted by Olsson in his talk at the MIT workshop [4].

TABLE I. Comparison of the predictions in $O(p^4)$ $S\chi$ PT and $G\chi$ PT for those subthreshold coefficients that we shall see, Sec. IV, can be reliably calculated dispersively, together with the results of Table II.

Coefficient	$S\chi$ PT $O(p^4)$	$G\chi$ PT $O(p^4)$	Dispersive result (Table II) $a_0^0=0.20$
$F_{1,0}^{(0)}$	1.76×10^{-2}	1.72×10^{-2}	$(1.6 \pm 0.2) \times 10^{-2}$
$\mu^2 F_{1,1}^{(0)}$	-2.07×10^{-3}	-2.21×10^{-3}	$-(2.1 \pm 0.3) \times 10^{-3}$
$F_{2,0}^{(0)}$	1.23×10^{-3}	1.42×10^{-3}	$(1.7 \pm 0.3) \times 10^{-3}$
$F_{1,0}^{(1)}$	1.08×10^{-3}	2.22×10^{-3}	$(2.5 \pm 0.4) \times 10^{-3}$
$\mu^2 F_{1,1}^{(1)}$	-0.51×10^{-3}	-1.18×10^{-3}	$-(1.1 \pm 0.2) \times 10^{-3}$
$F_{2,0}^{(1)}$	3.32×10^{-4}	7.88×10^{-4}	$(6.8 \pm 1.0) \times 10^{-4}$
$\mu^4 F_{0,2}^{(1)}$	1.87×10^{-4}	4.01×10^{-4}	$(4.8 \pm 0.8) \times 10^{-4}$
$F_{1,0}^{(2)}$	4.67×10^{-3}	4.33×10^{-3}	$(5.1 \pm 0.8) \times 10^{-3}$
$\mu^2 F_{1,1}^{(2)}$	-1.35×10^{-3}	-1.91×10^{-3}	$-(2.1 \pm 0.3) \times 10^{-3}$
$F_{2,0}^{(2)}$	0.78×10^{-3}	1.26×10^{-3}	$(1.3 \pm 0.2) \times 10^{-3}$
$\mu^4 F_{0,2}^{(2)}$	1.23×10^{-3}	1.27×10^{-3}	$(1.1 \pm 0.2) \times 10^{-3}$

just described. Ignoring the final column for the moment, we see that the values for $F_{1,0}^{(0)}$, $\mu^2 F_{1,1}^{(0)}$, $F_{2,0}^{(0)}$, $F_{1,0}^{(1)}$, and $\mu^4 F_{0,2}^{(1)}$, are in close agreement regardless of which version of χ PT is used. However, each of $F_{1,0}^{(1)}$, $\mu^2 F_{1,1}^{(1)}$, $F_{2,0}^{(1)}$, $\mu^4 F_{0,2}^{(1)}$, $\mu^2 F_{1,1}^{(2)}$, $F_{2,0}^{(2)}$ are predicted to differ by a factor of 2. Consequently, one may expect that if we can evaluate these from experiment, data could distinguish between the two versions of χ PT, at least to $O(p^4)$. It is to the evaluation of these *discriminatory* coefficients that we now turn.

IV. EVALUATION OF THE DISPERSIVE INTEGRALS: TEST A

The evaluation of the subthreshold coefficients according to test A consists of inputting experimental data for the $\pi\pi$ amplitudes with definite isospin in the t channel into the dispersive integrals for the subthreshold coefficients, Eqs. (8)–(12), as Chell and Olsson [4] did. However the experimental information in the very low energy region near threshold is still very poor [6]. Moreover, as we shall see, it is precisely this energy regime that is most important for the evaluation of the subthreshold coefficients. Consequently, we perform test A using a parametrization of the $\pi\pi$ amplitudes that reproduces the major features of the experimental data, as a way of restricting the uncertainties.

We calculate the dispersive integrals of Eqs. (8)–(12) by subdividing the energy range, E , where $s=E^2$, into three regions: (I) $2\mu \leq E \leq E_1$, the near threshold region; (II) $E_1 < E \leq E_2$, the intermediate energy region; (III) $E_2 < E$, the high energy region. E_1 is 0.8–0.9 GeV, while E_2 is chosen so that E_2^2 is halfway between the $\rho_3(1690)$ and $f_4(2050)$ resonance squared masses, in keeping with finite energy sum-rule phenomenology, i.e. $E_2=1.85$ GeV. As we shall see, for almost all the integrals of Eqs. (8)–(12), region III, where Regge behavior of the form given in Eqs. (5) applies, gives a negligible contribution. We use the Regge residues determined in Ref. [7]. In region II, the $f_2(1270)$ and $\rho_3(1690)$ contributions are included in the narrow resonance approximation and are also, for the most part, small. Region

I with $E_1=0.8$ –0.9 GeV generally dominates. In this region, only S and P waves need to be included. In terms of the phase shifts, $\delta_{\ell}^I(s)$, we have

$$\begin{aligned} \text{Im}F^{I_t=0}(s,t) &= \sqrt{\frac{s}{s-4\mu^2}} \left\{ \frac{1}{3} \sin^2 \delta_0^0(s) \right. \\ &\quad \left. + 3 \left(1 + \frac{2t}{s-4\mu^2} \right) \sin^2 \delta_1^1(s) + \frac{5}{3} \sin^2 \delta_0^2(s) \right\}, \\ \text{Im}F^{I_t=1}(s,t) &= \frac{4\mu^2}{2s+t-4\mu^2} \sqrt{\frac{s}{s-4\mu^2}} \left\{ \frac{1}{3} \sin^2 \delta_0^0(s) \right. \\ &\quad \left. + \frac{3}{2} \left(1 + \frac{2t}{s-4\mu^2} \right) \sin^2 \delta_1^1(s) - \frac{5}{6} \sin^2 \delta_0^2(s) \right\}, \end{aligned} \quad (47)$$

$$\begin{aligned} \text{Im}F^{I_t=2}(s,t) &= \sqrt{\frac{s}{s-4\mu^2}} \left\{ \frac{1}{3} \sin^2 \delta_0^0(s) \right. \\ &\quad \left. - \frac{3}{2} \left(1 + \frac{2t}{s-4\mu^2} \right) \sin^2 \delta_1^1(s) + \frac{1}{6} \sin^2 \delta_0^2(s) \right\}. \end{aligned}$$

In the low energy region the phase shifts may usefully be expanded in powers of momenta by

$$\delta_{\ell}^I(s) = \left(\frac{s-4\mu^2}{4\mu^2} \right)^{\ell+1/2} \left[a_{\ell}^I + b_{\ell}^I \left(\frac{s-4\mu^2}{4\mu^2} \right) + \dots \right], \quad (48)$$

where a_{ℓ}^I are the scattering lengths and b_{ℓ}^I the effective ranges. This near threshold expansion is naturally embodied in the following flexibly convenient representation of the phase shifts [8] in terms of the K matrix:

$$\begin{aligned} K_{\ell}^I &\equiv \sqrt{\frac{s}{s-4\mu^2}} \tan \delta_{\ell}^I(s) \\ &= \left(\frac{s-4\mu^2}{4\mu^2} \right)^{\ell} \left\{ a_{\ell}^I + \bar{b}_{\ell}^I \left(\frac{s-4\mu^2}{4\mu^2} \right) \right\} \frac{4\mu^2 - s_{\ell}^I}{s - s_{\ell}^I}, \\ \bar{b}_{\ell}^I &= b_{\ell}^I - a_{\ell}^I \left(\frac{4\mu^2}{s_{\ell}^I - 4\mu^2} \right) + (a_{\ell}^I)^3 \delta_{\ell 0}, \end{aligned} \quad (49)$$

where, as already mentioned, the a_{ℓ}^I , b_{ℓ}^I , and s_{ℓ}^I are fixed to give a parametrization consistent with experiment and with χ PT in its appropriate version. Other parametrizations have been tried and these alter our numbers little — this is a consequence of the integrals being dominated by the near threshold absorptive parts. To illustrate this, we show in Fig. 1, the integrands for $F_{k,m}^{(I)}$ as functions of energy $E = \sqrt{s}$ for two different values of the $I=0$ S -wave scattering length a_0^0 . One sees that the low energy region largely determines their dispersive evaluation, except for $F_{0,1}^{(1,2)}$.

In Table II, we present the contributions to the dispersive integrals in regions I, II, and III. In region I the S -wave parameters have been fixed to those determined by Schenk [8], which represent the well-known experimental results re-

TABLE II. Contribution to the subthreshold coefficients Eqs. (8)–(12) from the three different energy regions as explained in the text. Typical uncertainties are 15%, 10%, 25%, respectively, in these three contributions.

Coefficient	Region I	Region II	Region III	Total
$F_{1,0}^{(0)}$	1.56×10^{-2}	3.46×10^{-4}	2.54×10^{-4}	1.6×10^{-2}
$\mu^2 F_{1,1}^{(0)}$	-2.19×10^{-3}	2.09×10^{-5}	1.63×10^{-5}	-2.1×10^{-3}
$F_{2,0}^{(0)}$	1.67×10^{-3}	1.92×10^{-7}	1.10×10^{-8}	1.7×10^{-3}
$F_{1,0}^{(1)}$	2.52×10^{-3}	6.96×10^{-6}	5.30×10^{-7}	2.5×10^{-3}
$\mu^2 F_{0,1}^{(1)}$	-1.46×10^{-3}	9.57×10^{-4}	2.00×10^{-3}	Unreliable
$\mu^2 F_{1,1}^{(1)}$	-1.08×10^{-3}	4.05×10^{-7}	3.65×10^{-8}	-1.1×10^{-3}
$F_{2,0}^{(1)}$	6.79×10^{-4}	4.34×10^{-9}	3.81×10^{-11}	6.8×10^{-4}
$\mu^4 F_{0,2}^{(1)}$	3.86×10^{-4}	8.78×10^{-6}	9.12×10^{-5}	4.8×10^{-4}
$F_{1,0}^{(2)}$	4.88×10^{-3}	2.29×10^{-4}	$\sim 10^{-5}$	5.1×10^{-3}
$\mu^2 F_{0,1}^{(2)}$	-3.98×10^{-2}	1.39×10^{-2}	$\sim 10^{-2}$	Unreliable
$\mu^2 F_{1,1}^{(2)}$	-2.12×10^{-3}	1.25×10^{-5}	$\sim 10^{-6}$	-2.1×10^{-3}
$F_{2,0}^{(2)}$	1.25×10^{-3}	1.70×10^{-7}	$\sim 10^{-8}$	1.3×10^{-3}
$\mu^4 F_{0,2}^{(2)}$	1.13×10^{-3}	-1.00×10^{-5}	$\sim 10^{-5}$	1.1×10^{-3}

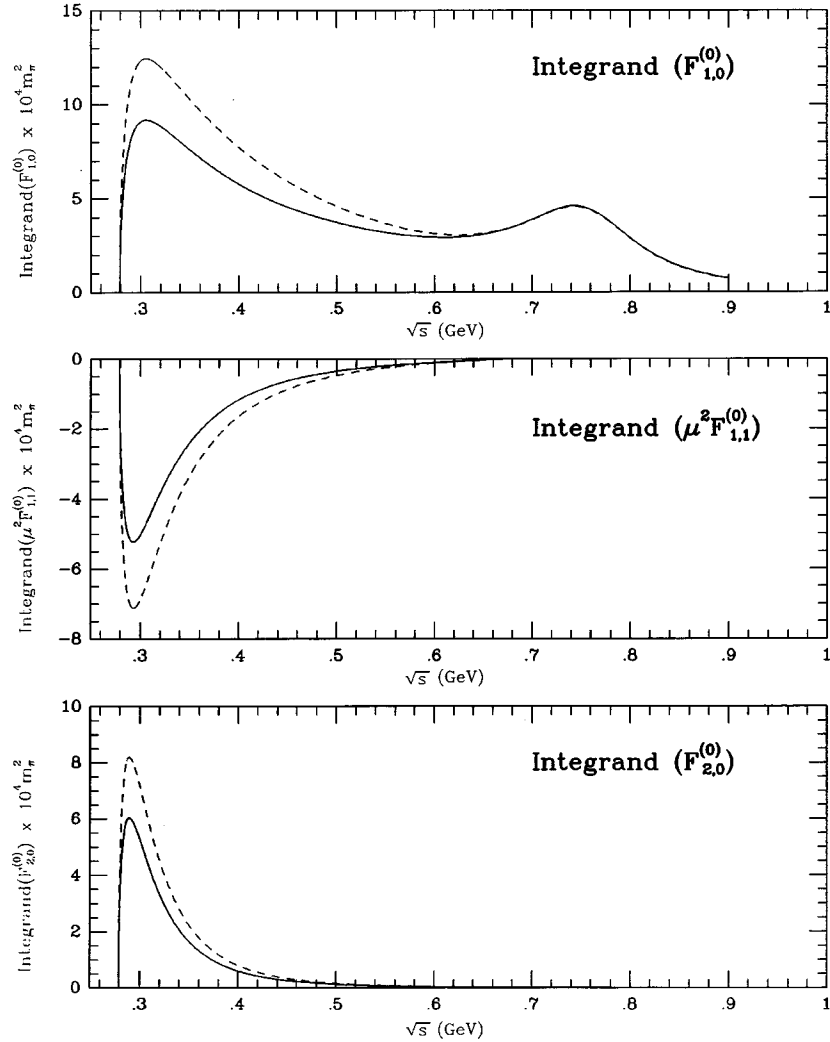


FIG. 1. Integrands of the dispersion relations for $F_{k,m}^{(l)}$ as in Eqs. (8)–(12), in energy region I as a function of \sqrt{s} evaluated using Eqs. (49) and (47) with $a_0^0=0.20$ (solid lines) and $a_0^0=0.27$ (dashed lines). The ordinate is given in arbitrary dimensionless units.

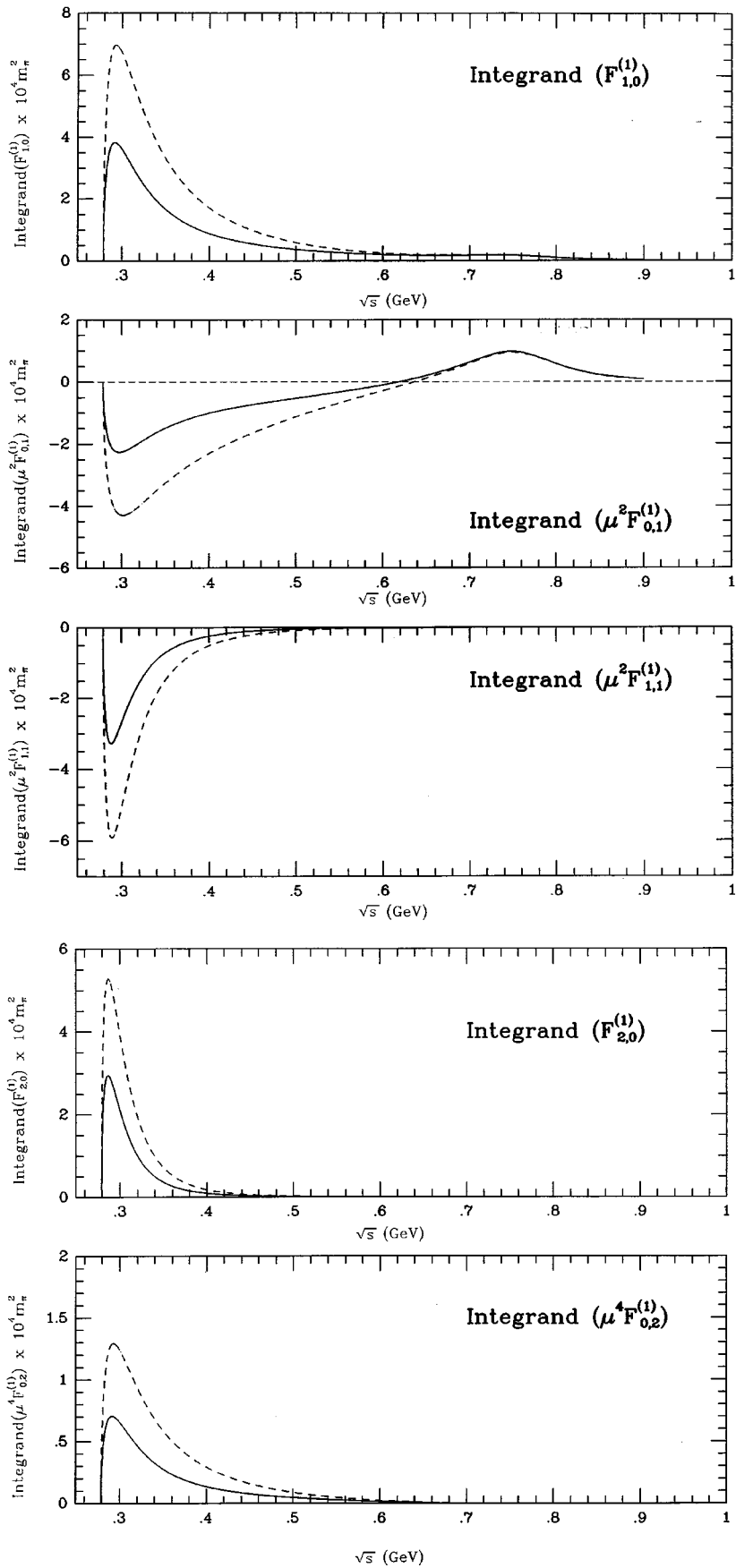


FIG. 1 (Continued).

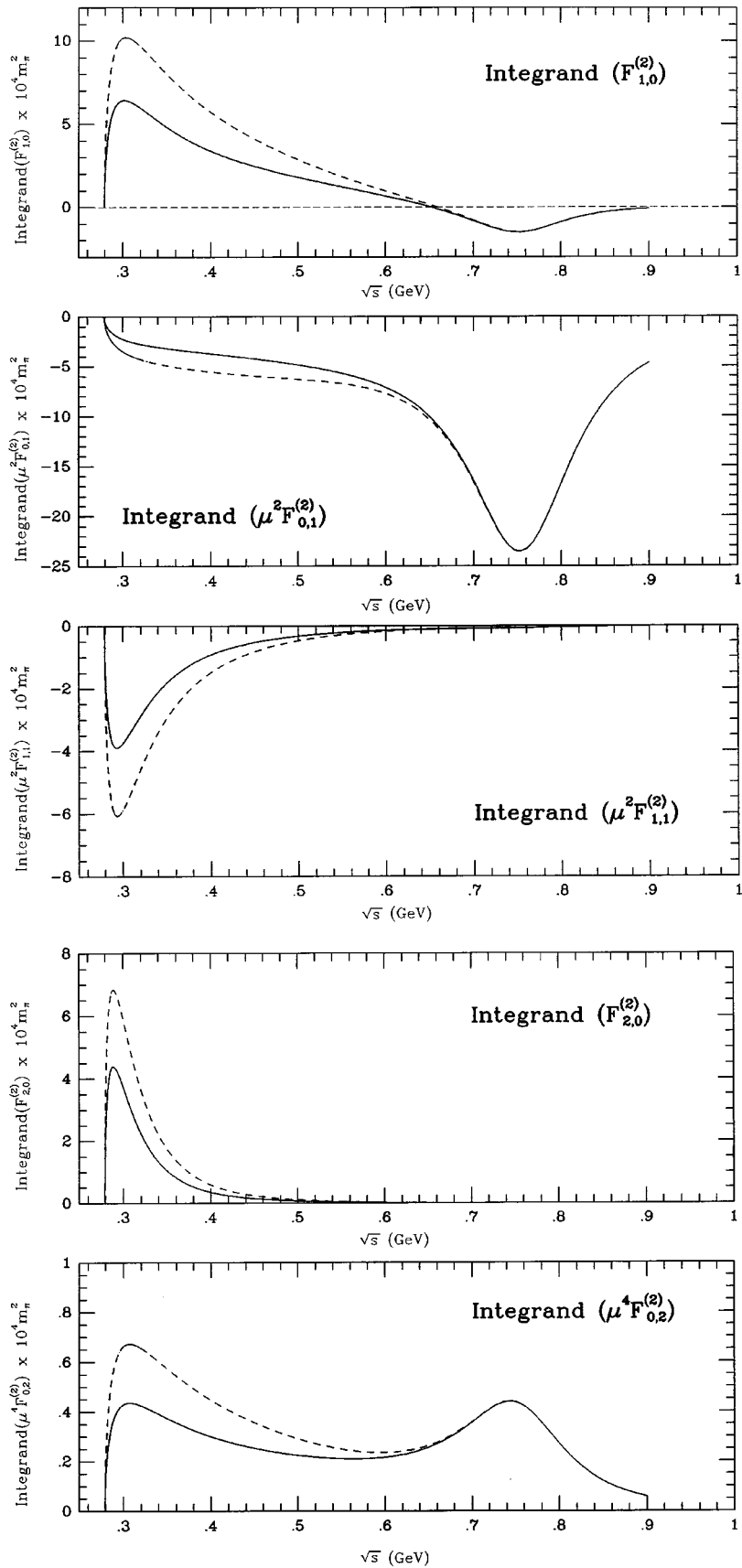


FIG. 1 (Continued).

TABLE III. Comparison of the results for those subthreshold coefficients that can be reliably calculated dispersively, with $a_0^0=0.16$ and 0.23 , with their predictions in $S\chi$ PT and $G\chi$ PT at $O(p^4)$.

Coefficient	$S\chi$ PT $O(p^4)$	Dispersive results $a_0^0=0.16$	$G\chi$ PT $O(p^4)$	Dispersive results $a_0^0=0.23$
$F_{1,0}^{(0)}$	1.76×10^{-2}	$(1.4 \pm 0.2) \times 10^{-2}$	1.72×10^{-2}	$(1.4 \pm 0.2) \times 10^{-2}$
$\mu^2 F_{1,1}^{(0)}$	-2.07×10^{-3}	$-(1.5 \pm 0.3) \times 10^{-3}$	-2.21×10^{-3}	$-(1.8 \pm 0.4) \times 10^{-3}$
$F_{2,0}^{(0)}$	1.23×10^{-3}	$(1.3 \pm 0.3) \times 10^{-3}$	1.42×10^{-3}	$(1.5 \pm 0.3) \times 10^{-3}$
$F_{1,0}^{(1)}$	1.08×10^{-3}	$(1.5 \pm 0.3) \times 10^{-3}$	2.22×10^{-3}	$(2.6 \pm 0.4) \times 10^{-3}$
$\mu^2 F_{1,1}^{(1)}$	-0.51×10^{-3}	$-(0.6 \pm 0.1) \times 10^{-3}$	-1.18×10^{-3}	$-(1.2 \pm 0.3) \times 10^{-3}$
$F_{2,0}^{(1)}$	3.32×10^{-4}	$(3.7 \pm 0.6) \times 10^{-4}$	7.88×10^{-4}	$(8.2 \pm 0.5) \times 10^{-4}$
$\mu^4 F_{0,2}^{(1)}$	1.87×10^{-4}	$(2.0 \pm 0.5) \times 10^{-4}$	4.01×10^{-4}	$(4.0 \pm 0.4) \times 10^{-4}$
$F_{1,0}^{(2)}$	4.67×10^{-3}	$(2.6 \pm 0.6) \times 10^{-3}$	4.33×10^{-3}	$(3.9 \pm 0.6) \times 10^{-3}$
$\mu^2 F_{1,1}^{(2)}$	-1.35×10^{-3}	$-(1.4 \pm 0.2) \times 10^{-3}$	-1.91×10^{-3}	$-(2.0 \pm 0.4) \times 10^{-3}$
$F_{2,0}^{(2)}$	0.78×10^{-3}	$(0.8 \pm 0.1) \times 10^{-3}$	1.26×10^{-3}	$(1.3 \pm 0.2) \times 10^{-3}$
$\mu^4 F_{0,2}^{(2)}$	1.23×10^{-3}	$(1.0 \pm 0.2) \times 10^{-3}$	1.27×10^{-3}	$(1.1 \pm 0.2) \times 10^{-3}$

viewed in [6] and match one loop $S\chi$ PT near threshold, i.e., we take $\mu = 139.6$ MeV, $a_0^0 = 0.20$, $b_0^0 = 0.24$, $s_0^0 = (0.865 \text{ GeV})^2$, $a_0^2 = -0.042$, $b_0^2 = -0.075$, $s_0^2 = -(0.685 \text{ GeV})^2$. For the P wave we take $a_1^1 = 0.037$, $b_1^1 = 0.005$, and $s_1^1 = (0.77 \text{ GeV})^2$, the squared ρ mass. The uncertainties are typically 10% in region II, 25% in region III and, even keeping a_0^0 fixed at its $O(p^4)$ χ PT value, $\sim 15\%$ in region I. With these uncertainties, the dispersive results of Table II are added as the last column in Table I. One now sees that the coefficients for which $S\chi$ PT and $G\chi$ PT predicted a common value, agree well with their dispersive evaluation from experiment. In contrast, the so-called *discriminatory* coefficients, that generally differ by a factor of 2 at $O(p^4)$, are far closer to the predictions of $G\chi$ PT (with $\alpha = 3.1$, $\beta = 0.93$) than with $S\chi$ PT. This is at first sight rather surprising since the input absorptive parts have been explicitly designed (by Schenk [8]) to match $O(p^4)$ $S\chi$ PT. In contrast, the coefficients in $G\chi$ PT to $O(p^4)$ are in very good agreement with the same dispersive evaluation. If this were the whole story then this would indicate that low orders in $G\chi$ PT more rapidly embody key resonance contributions.

However, let us return to the evaluation of the *discriminatory* coefficients from experimental information. In Fig. 1 we see that all the *discriminatory* coefficients are entirely dominated by the very near threshold region below 450 MeV or so and though the values given in column fourth of Table I have 15% errors, this is assuming a particular value of the $l=0$ S -wave scattering length, $a_0^0 = 0.20$ in Eq. (49). If we fold in the real uncertainties from the Geneva-Saclay K_{e4} results [9] on the near threshold phase shifts, then one would readily see that for these coefficients the present experimental uncertainties are more than 100% [6] (compare the two curves in Fig. 1) encompassing both $S\chi$ PT and what we call $G\chi$ PT in Table I. Thus experiment cannot presently distinguish between these differing versions of χ PT and so test A is inconclusive. Nonetheless, the Chell-Olsson test in form B does tell us that the $O(p^6)$ corrections in $S\chi$ PT must be large, as we discuss next.

V. WHEN IS THE CHELL-OLSSON TEST AN IDENTITY (TEST B)?

For the *discriminatory* coefficients, the dispersive integrals are controlled by the near threshold region where we

would expect χ PT should itself be applicable. Then these relations should be an identity, since the amplitudes of χ PT satisfy the crossing and analyticity properties that Eqs. (6) and (7) embody. Thus if we evaluate the subthreshold coefficients directly from χ PT in either form at $O(p^4)$, for example, or alternatively input the $O(p^4)$ imaginary parts into the dispersive integrals for $F_{k,m}^{(l)}$, Eqs. (8)–(12), the results should be the same. However, comparing columns 2 and 4 of Table I, we see that inputting phases with the $O(p^4)$ S -wave scattering length of $a_0^0 = 0.20$ does not reproduce $S\chi$ PT. This is because χ PT only satisfies unitarity perturbatively. Consistency with the $O(p^4)$ subthreshold coefficients requires the $O(p^4)$ imaginary parts be input into the dispersive integrals. This $O(p^4)$ absorptive part is wholly given by the $O(p^2)$ real part, since

$$\text{Im}f_{\ell}^l(s, O(p^4)) = \sqrt{1 - \frac{4\mu^2}{s}} [\text{Re}f_{\ell}^l(s, O(p^2))]^2. \quad (50)$$

Thus the Chell-Olsson test should become an identity, if we input phases at the appropriate order. Working to $O(p^4)$ for the coefficients, we must input phases at $O(p^2)$ for which $a_0^0 = 0.16$ in $S\chi$ PT or $a_0^0 = 0.23$ in our version of $G\chi$ PT with $\alpha = 3.1$. With these values we obtain the results in Table III.

We now see complete agreement between the dispersive results and the explicit evaluation (except for $F_{1,0}^{(2)}$ which appears to be due to a poorer convergence in the dispersive evaluation). The fact that the discriminatory coefficients in $S\chi$ PT and $G\chi$ PT differ by a factor 2 at $O(p^4)$ just reflects the fact that the imaginary parts of the near threshold amplitudes are very nearly proportional to $(a_0^0)^2$ and $(0.23/0.16)^2 \approx 2.1$. Moreover, the large change in the *discriminatory* coefficients in $S\chi$ PT between their values in column 2 of Table III and column 2 of Table I means that the $O(p^6)$ corrections must be large—since inputting $O(p^4)$ phases in Table I generates $O(p^6)$ coefficients. The recent two-loop calculation of the $\pi\pi$ amplitude by Bijnens *et al.* [10] bears this out, as Moussallam has checked.⁴ In Table IV

⁴B. Moussallam (private communication).

TABLE IV. Comparison between the $S\chi$ PT evaluation at $O(p^4)$, $O(p^6)$ and the dispersive calculation for $a_0^0=0.20$ of two of the *discriminatory* coefficients. The $O(p^6)$ $S\chi$ PT computation was made by Moussallam (see footnote 4).

Coefficient	$S\chi$ PT $O(p^4)$	$S\chi$ PT $O(p^6)$	Dispersive ($a_0^0=0.20$)
$F_{1,0}^{(1)} \times 10^3$	1.08	2.51	(2.5 ± 0.4)
$\mu^2 F_{1,1}^{(1)} \times 10^3$	-0.51	-0.95	$-(1.1 \pm 0.2)$

we give examples of the change at $O(p^6)$, for $F_{1,0}^{(1)}$ and $F_{1,1}^{(1)}$. The self-consistency is now clear after these 100% corrections.

The fact that the $O(p^6)$ $I=0$ S -wave scattering length differs by 8% from its $O(p^4)$ value in $S\chi$ PT [10], allows us to estimate that the *discriminatory* coefficients will have just a 17% correction at $O(p^8)$ and so the Standard perturbative expansion is improving.

VI. CONCLUSIONS

The Chell-Olsson test is indeed stringent. However, using presently available experimental information, it is not able to distinguish between $S\chi$ PT and $G\chi$ PT. This reflects the large uncertainties in the near threshold S -wave phases that hopefully measurements of K_{e4} decays with higher statistics and smaller systematic uncertainties at $DA\Phi$ NE will improve.

The coefficients in the subthreshold expansion that have the most potential to distinguish both forms of χ PT, the ones

we have called *discriminatory*, all have no polynomial $O(p^4)$ corrections in terms of the $\bar{\mathcal{L}}_i$'s of $S\chi$ PT. Curiously enough we have shown that these same coefficients have $\sim 100\%$ corrections at $O(p^6)$ and the recent explicit calculation of Bijmens *et al.* [10] of the two-loop $\pi\pi$ amplitude shows that is, in fact, so. Indeed, these same calculations and our study allow an estimate of $\sim 17\%$ to be made for the $O(p^8)$ corrections to these subthreshold coefficients. Thus the Chell-Olsson test becomes an identity when applied to the amplitudes of χ PT. This is because they have the crossing and analytic properties of the full amplitude provided we recognize that unitarity is only satisfied perturbatively—order by order.

ACKNOWLEDGMENTS

This collaboration was made possible by the support of the EC Human Capital and Mobility Programme which funds the EURODAΦNE network under Grant No. CHRX-CT920026. J.P. wishes to thank the Particle Physics Department of the Rutherford-Appleton Laboratory, where this work was started, for their kind hospitality. We are grateful to Gilberto Colangelo, Jürg Gasser, Marc Knecht, and Jan Stern for discussions and particularly to Bachir Moussallam for his evaluation of the coefficients in two-loop $S\chi$ PT. We are also grateful to Hans Bijmens and Ulf-G. Meissner for the opportunity to present this work at the ECT* *Workshop on the Standard Model at Low Energies* at Trento. J.P. was also partially supported by DGICYT under Grant No. PB94-0080.

-
- [1] P. Gensini, N. Paver, and C. Verzegnassi, Phys. Lett. **47B**, 515 (1973); C. B. Lang and W. Porod, Phys. Rev. D **21**, 1295 (1980); V. Bernard, N. Kaiser, and Ulf-G. Meissner, Nucl. Phys. **B357**, 129 (1991).
- [2] J. Gasser and H. Leutwyler, Ann. Phys. (N.Y.) **158**, 142 (1984); Nucl. Phys. **B250**, 465 (1985).
- [3] J. Stern, H. Sazdjian, and N. H. Fuchs, Phys. Rev. D **47**, 3814 (1993); M. Knecht and J. Stern, in *The Second DAΦNE Physics Handbook*, edited by L. Maiani, G. Pancheri, and N. Paver (INFN, Frascati, 1995), pp. 169–190.
- [4] M.G. Olsson, in *Proceedings of the Workshop on Chiral Dynamics: Theory and Experiment*, Cambridge, 1994, Lecture Notes in Physics, LNP 452, edited by A.M. Bernstein and B.R. Holstein (Springer-Verlag, Berlin, 1995), p. 111.
- [5] M. Knecht, B. Moussallam, and J. Stern, in *The Second DAΦNE Physics Handbook* [3], pp. 221–236.
- [6] D. Morgan and M. R. Pennington, in *The Second DAΦNE Physics Handbook* [3], pp. 193–213.
- [7] M. R. Pennington, Ann. Phys. (N.Y.) **92**, 164 (1975).
- [8] A. Schenk, Nucl. Phys. **B363**, 97 (1991).
- [9] L. Rosselet *et al.*, Phys. Rev. D **15**, 574 (1977).
- [10] J. Bijmens, G. Colangelo, G. Ecker, J. Gasser, and M. Sainio, Phys. Lett. B **374**, 210 (1996).